# Phase Noise Characterization of SAW Oscillators Based on a Newton Minimization Procedure

David P. Klemer, *Member, IEEE*, Ko-Ming Shih, *Member, IEEE*, and Earl E. Clark III, *Member, IEEE*

*Abstract*—**An iterative minimization technique is used to optimize the values of circuit and device parameters which determine the phase noise response of a voltage-controlled SAW-stabilized oscillator (VCSO). An expression developed by Parker is used to calculate the double-sideband phase noise to carrier ratio from circuit parameter values; good agreement between calculations and phase noise measurements is achieved by minimizing the squared error through the use of a steepest-descent/Newton–Raphson minimization scheme. Less accurately known circuit parameters are thus optimized in an iterative fashion. Exact expressions for the elements of the Hessian matrix are used in the Newton–Raphson procedure, allowing for fast computations.**

**Although this technique is primarily useful in the determination of circuit parameter values, it can also be used to develop an understanding of the effect of individual parameters on phase noise response (i.e., the sensitivity of phase noise characteristics to circuit and device parameter variations). Additionally it may be of use in the design of low-phase-noise oscillators by using desired (rather than measured) phase noise values in the objective function to be minimized.**

## I. Introduction

An understanding of the sources of phase noise in microwave oscillators becomes important as phase noise specifications become increasingly stringent in state-of-the-art radar and navigation systems. The requirements for lower phase noise levels have led to current interest in describing and understanding the sources of frequency fluctuations in resonator-stabilized oscillators [1], [2]. For example, the sources of so-called $1/f$ or flicker noise in SAW-stabilized oscillators have been the subject of recent investigation; this noise phenomenon predominates in most SAW devices [3]. An expression developed by Parker can be used to predict the double-sideband phase noise to carrier ratio for a SAW-resonator-based oscillator [4], [5]:

$$S_\phi(f_m) = \left[\frac{\alpha_R f_o^4}{f_m^3}\right] + \left[\frac{\alpha_E}{(2\pi\tau_g)^2 f_m^3}\right] + \left[\frac{2\alpha_R Q_L f_o^3}{f_m^2}\right] + \left[\frac{2GFKT/P_o}{(2\pi\tau_g)^2 f_m^2}\right] + \frac{\alpha_E}{f_m} + \frac{2GFKT}{P_o} \quad (1)$$

where $f_m$ is the carrier offset frequency. In this equation, $G$ and $F$ are the compressed power gain and noise factor, respectively, of the oscillator loop amplifier; $f_o$ and $P_o$ are respectively the carrier frequency and power level at the loop amplifier output. The SAW device is characterized by the parameters $\tau_g$, $Q_L$, and $\alpha_R$, which are respectively the SAW group delay, the loaded $Q$ ($= \pi f_o \tau_g$), and the flicker noise constant. The constant $\alpha_E$ is the flicker noise constant of the loop amplifier, and $K$ and $T$ are respectively Boltzmann's constant and the temperature in degrees Kelvin. In practice, $\alpha_R$ and $\alpha_E$ are determined from open-loop phase noise measurements of the SAW device and loop amplifier [6]. Fig. 1 illustrates the circuit topology under consideration; a feedback loop formed by a voltage-variable phase shifter in series with a resonant SAW device is used to adjust the oscillation frequency. The transmission characteristics of a typical SAW device are also shown.

If sufficiently accurate estimates of parameter values are available, the Parker expression can be used to calculate the phase noise characteristic of a SAW-based oscillator. In general, however, inaccuracy in the estimated values of the parameters will lead to discrepancy between the calculated values and values measured on a phase noise measurement system. This inaccuracy may arise from the difficulty in characterizing open-loop phase noise response for passive loop components such as the SAW resonator or the difficulty in inferring precise parameter values under closed-loop (large-signal) operating conditions.

It is possible to use a carefully measured phase noise characteristic to determine accurate values for less accu-

Manuscript received September 24, 1990; revised January 3, 1991. This work was supported by RF Monolithics, Inc., and by the National Science Foundation Industry/University Cooperative Research Center for Advanced Electron Devices and Systems at the University of Texas at Arlington.

D. P. Klemer is with the Department of Electrical Engineering, University of Texas at Arlington, Box 19016, Arlington, TX 76019.

K.-M. Shih was with the Department of Electrical Engineering, University of Texas at Arlington. He is now with the Department of Electrical and Computer Engineering, Mercer University, Macon, GA 31207.

E. E. Clark III is with RF Monolithics, Inc., 4441 Sigma Road, Dallas, TX 75244.

IEEE Log Number 9143688.

0018-9480/91/0500-0883$01.00 ©1991 IEEE

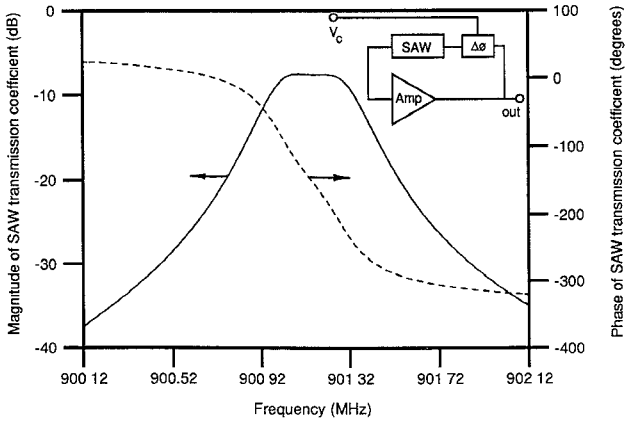


Fig. 1. Voltage-controlled SAW oscillator block diagram and typical SAW transmission characteristics.

rately known values of the circuit and device parameters. Our approach has been to employ an iterative technique to minimize a nonlinear function which expresses the squared error between measured phase noise values and values computed using (1). In Section II we describe the formulation and implementation of our algorithm and discuss the numerical considerations which led to the specific choice of the squared-error function. We also describe an alternative form of (1) which is useful in understanding the circuit- and device-related contributions to phase noise behavior. In Section III we present examples of calculations performed using the algorithm, including graphical illustrations of objective function error as a function of frequency and circuit parameters.

## II. Formulation of the Algorithm

### A. The Squared-Error Function

Consider the error function

$$\varphi(\boldsymbol{x}) = \sum_{i=1}^{N} \left[ S_\phi(f_i, \boldsymbol{x}) - \hat{S}(f_i) \right]^2 \tag{2}$$

where the first term in the brackets, $S_\phi$, represents the calculated value of phase noise to carrier ratio using (1) and the second term, $\hat{S}$, represents the phase noise values measured at $N$ discrete frequencies $f_i$, $i = 1, \cdots, N$. The vector $\boldsymbol{x}$ consists of those parameters $x_k$, $k = 1, \cdots, M$, which are to be accurately determined using the iterative minimization scheme, for example $\alpha_R$, $\alpha_E$, and the loop amplifier noise factor, $F$.

In the usual fashion, we can minimize the error function, $\varphi(\boldsymbol{x})$, by locating the point in parameter space where the gradient vector of (2) vanishes [7]:

$$\boldsymbol{g}(\boldsymbol{x}) = \boldsymbol{0} \tag{3}$$

where

$$\boldsymbol{g}(\boldsymbol{x}) \equiv \left[ \frac{\partial \varphi}{\partial x_1}, \cdots, \frac{\partial \varphi}{\partial x_M} \right]^T. \tag{4}$$

A Newton–Raphson iteration is used to drive the gradient vector to zero: an updated estimate for the parameter vector $\boldsymbol{x}$, $\boldsymbol{x}_{v+1}$, is derived from the original parameter estimate $\boldsymbol{x}_v$ as

$$\boldsymbol{x}_{v+1} = \boldsymbol{x}_v - \boldsymbol{G}^{-1}(\boldsymbol{x}_v)\boldsymbol{g}(\boldsymbol{x}_v) \tag{5}$$

where the symmetric Hessian matrix, $\boldsymbol{G}(\boldsymbol{x})$, is

$$\boldsymbol{G}(\boldsymbol{x}) = \left[ \frac{\partial^2 \varphi}{\partial x_i \partial x_j} \right], \qquad i, j = 1, \cdots, M. \tag{6}$$

Expressions for the gradient vector and for the elements of the Hessian matrix will be presented shortly.

Because the Newton–Raphson technique may be slow to converge if the initial estimate is far from the error function minimum, it is helpful to employ an alternative minimization scheme for the initial phases of the minimization process. The steepest-descent method uses the negative of the gradient vector (4) to indicate the direction of the maximum decrease in the error function. An updated estimate for the parameter vector $\boldsymbol{x}$ is derived from the original parameter estimate, $\boldsymbol{x}_v$, as

$$\boldsymbol{x}_{v+1} = \boldsymbol{x}_v - k_v \cdot \boldsymbol{g}(\boldsymbol{x}_v) \tag{7}$$

where $k_v$ is an appropriate scaling factor. In practice, a combination of steepest-descent and Newton–Raphson techniques may be used to effect an efficient function minimization.

At this point, it is important to recognize that there are two crucial assumptions involved in the valid application of this algorithm: (i) the phase noise values $\hat{S}(f_i)$ are indeed accurate measurements of the actual phase noise of the oscillator under test and are uncorrupted by effects of measurement instrumentation noise; and (ii) the equation (1) provides an accurate description of the phase noise phenomenology for the oscillator being characterized.

Regarding the first point, the accuracy of the phase noise measurements depends upon many factors, for example, the measurement technique employed (frequency discriminator, two-source, three-source, or direct spectrum analyzer measurement) and the noise levels inherent in the instrumentation hardware. In the two-source technique, for example, a noisy reference source contributes an error in the noise measurement given by Error (dB) = $10\log(1 + P_{\text{ref}}/P_{\text{osc}})$, where $P_{\text{osc}}$ is the actual oscillator noise power and $P_{\text{ref}}$ is the actual noise power generated in the reference oscillator [8]. An estimate can thus be derived for the instrumentation-induced error in the phase noise measurements, and from this estimate a study of the worst-case errors expected in the parameter vector $\boldsymbol{x}$ can be conducted. More comprehensive approaches for determining worst-case uncertainty associated with various phase noise measurement techniques are readily available from manufacturers of phase noise measurement instrumentation [9], [10].

Regarding the application of (1), a number of assumptions are implicit in the development of this expression, for example, the effect of in-band and out-of-band SAW

impedance variation on such circuit parameters as loop amplifier noise factor. (In the case of the SAW oscillator studied later, resistive loss was used to mitigate the effects of out-of-band SAW impedance variations.) A model for the SAW-stabilized feedback-loop oscillator was originally described by Leeson [11] in 1966 and used by Parker and Montress [6] in the derivation of (1). It is important to note—as indicated in Parker [4]—that the oscillator loop amplifier is presented with an identical equivalent generator impedance (i.e., feedback device impedance) for both open-loop and closed-loop measurements used to determine the various circuit and device parameters. An extensive development of (1) is available in the literature, including effects of circuit topology and impedance matching on the parameters involved (see, for example, [4, p. 102]). The reader should consult the references to obtain a thorough appreciation of the assumptions implicit in (1).

Let us now reconsider the specific form of the error function (2). Although the procedure for determining an optimum parameter set $\boldsymbol{x}$ by minimizing (2) is theoretically sound, the very high dynamic range of phase noise values encountered in practice (10 to 15 orders of magnitude) results in unacceptable numerical difficulty. For example, circuit and device effects far from the carrier frequency would be masked by "close-in" effects which would numerically dominate, owing to truncation and rounding errors.

For this reason, it is expedient to modify (2) logarithmically as follows:

$$\tilde{\varphi}(\boldsymbol{x}) = \sum_{i=1}^{N} \left\{ \hat{S}_{\mathrm{dB}}(f_i) - 10 \cdot \log_{10}\left[\frac{S_\phi(f_i, \boldsymbol{x})}{2}\right] \right\}^2 \tag{8}$$

where the measured phase noise values, $\hat{S}_{\mathrm{dB}}$, are now expressed in terms of decibels relative to the carrier level in a 1 Hz bandwidth (dBc/Hz), and the computed values are also converted to the same units. (Our nomenclature for phase noise to carrier ratio, $\hat{S}_{\mathrm{dB}}(f)$, is also commonly denoted as $\mathscr{L}(f)$). This modification serves to ameliorate numerical difficulties. Minimizing (8) minimizes the squared error between the measurements (in dBc/Hz) and the calculated values; increasing the exponent from 2 to a large number would result in a minimization in the minimax sense.

Calculation of the elements of the gradient vector is straightforward. Differentiating (8) gives

$$\frac{\partial \tilde{\varphi}(\boldsymbol{x})}{\partial x_k} = \sum_{i=1}^{N} 2 \cdot \left[ \hat{S}_{\mathrm{dB}}(f_i) - 10 \cdot \log_{10}\left(\frac{S_\phi(f_i, \boldsymbol{x})}{2}\right) \right] \cdot \left( \frac{-10 \cdot \dfrac{\partial S_\phi}{\partial x_k}}{\ln 10 \cdot S_\phi} \right) \tag{9}$$

where the derivatives of (1) are evaluated for the specific parameters to be optimized. For example, if we consider the flicker noise constants $\alpha_R$ and $\alpha_E$ and the loop amplifier noise factor, $F$, then the appropriate derivatives of $S_\phi$ are

$$\frac{\partial S_\phi}{\partial \alpha_R} = \frac{2Q_L f_o^3}{f_i^2} + \frac{f_o^4}{f_i^3} \tag{10}$$

$$\frac{\partial S_\phi}{\partial \alpha_E} = \frac{1}{(2\pi\tau_g)^2 f_i^3} + \frac{1}{f_i} \tag{11}$$

and

$$\frac{\partial S_\phi}{\partial F} = \frac{2GKT}{P_o}\left[1 + \frac{1}{(2\pi\tau_g)^2 f_i^2}\right]. \tag{12}$$

Here the derivatives are evaluated at a specific offset frequency $f_i$. The elements of the Hessian matrix can also be computed explicitly:

$$\frac{\partial^2 \tilde{\varphi}}{\partial x_j \partial x_k} = \frac{-20}{\ln 10} \sum_{i=1}^{N} \frac{-10S'(x_j)S'(x_k)}{(\ln 10)S^2} + \left(\hat{S}_{\mathrm{dB}} - \left(\frac{10}{\ln 10}\right)\ln\frac{S}{2}\right) \cdot \frac{SS''(x_j x_k) - S'(x_j)S'(x_k)}{S^2} \tag{13}$$

where $S$ is the value computed from (1), $S'$ represents the first partial derivative of (1) with respect to the parameter in parentheses, and $S''$ represents the second partial derivative with respect to the parameters indicated. The function $S$ and its derivatives are all functions of frequency $f_i$; for clarity, however, the summation index has been omitted in those terms above.

### *B. Implementation of the Minimization*

Equation (8) was derived to prevent numerical difficulty owing to the wide dynamic range in phase noise values. Additionally, it is helpful to note that the parameters to be determined also vary over a wide dynamic range: for example, $\alpha_R$ is of the order of $10^{-38}$ whereas $F$ may lie in the range 1–100. For this reason, it is beneficial to scale the parameters of interest in (1). If we express $f_o$ in GHz and $\tau_g$ in $\mu$s, and if we scale $\alpha_R$ and $\alpha_E$ by factors of $10^{38}$ and $10^{12}$ respectively, then we can rewrite (1) as

$$S_\phi(f_m) = \left[\frac{\alpha_R f_o^4}{f_m^3} \cdot 10^{-2}\right] + \left[\frac{\alpha_E}{(2\pi\tau_g)^2 f_m^3}\right] + \left[\frac{2\alpha_R Q_L f_o^3}{f_m^2} \cdot 10^{-11}\right] + \left[\frac{2GFKT/P_o}{(2\pi\tau_g)^2 f_m^2} \cdot 10^{12}\right] + \left[\frac{\alpha_E}{f_m} \cdot 10^{-12}\right] + \frac{2GFKT}{P_o} \tag{14}$$

where the variables discussed above now assume scaled values, including $Q_L (= \pi f_o \tau_g)$, which must also be scaled by a factor of $10^{-3}$. The derivatives of $S_\phi$ in (9) must be

modified accordingly when the scaled parameter values are being used.

The iteration proceeds by first selecting a best estimate of the parameter vector $\boldsymbol{x}$ from measurements of the components which comprise the voltage-controlled oscillator [4]. The appropriate derivatives of $S$ are computed (from (10)–(12), for example) as are the elements of the gradient vector $\boldsymbol{g}(\boldsymbol{x})$ given by (9).

At this point, if a steepest-descent approach is used, (7) allows the determination for an improved estimate for the parameter vector $\boldsymbol{x}$. The constant $k_v$ can be determined by estimating a value which locates the function minimum along the gradient direction; we used a less elegant approach wherein $k_v$ was chosen so that the greatest change in any parameter value did not exceed 50%. This approach was successful and did not appear to result in a significant increase in computation time.

As a function minimum is approached (noted when the incremental change in parameter values decreases), our algorithm switches to the Newton–Raphson technique. The elements (13) of the Hessian matrix $\boldsymbol{G}$ are computed and used to derive an improved estimate of the parameter vector using (5). The iteration then repeats until an error criterion is satisfied; in our case we iterate until the $L_2$ norm of $\boldsymbol{g}(\boldsymbol{x})$ falls below a given tolerance. For the parameter set $\boldsymbol{x}=[\alpha_R, \alpha_E, F]^T$ we note that the second partial derivatives are zero in the expression for the Hessian elements (13).

The matrix inverse of $\boldsymbol{G}$ in (5) can be calculated analytically if only a few parameters are being considered. However if $\boldsymbol{x}$ is composed of many parameters, then it is best to replace (5) with

$$\boldsymbol{G}(\boldsymbol{x}_v)\cdot\Delta\boldsymbol{x} = -\boldsymbol{g}(\boldsymbol{x}_v) \tag{15}$$

where $\Delta\boldsymbol{x} \equiv \boldsymbol{x}_{v+1} - \boldsymbol{x}_v$. Equation (15) is solved for $\Delta\boldsymbol{x}$ (and thus $\boldsymbol{x}_{v+1}$) using a standard matrix equation solver. Again, because the parameters involved exhibit a wide dynamic range it is usually necessary to normalize parameters as in (14) and/or to employ a matrix pivoting scheme in the numerical routine which solves (15) for $\Delta\boldsymbol{x}$.

### C. An Alternative Expression for $S_\phi$

The flicker noise constants $\alpha_R$ and $\alpha_E$ in (1) have a similar dominant effect on the close-in phase noise behavior for a SAW-stabilized oscillator owing to the $(f_m)^{-3}$ dependence. The similarity can be more clearly seen if one considers the expressions used to estimate these constants. From an open-loop phase noise measurement of the amplifier, $S'_{\phi E}(f_m)$, one can calculate $\alpha_E$ from

$$\alpha_E = f_m S'_{\phi E}(f_m). \tag{16}$$

Similarly, the constant $\alpha_R$ is computed from an open-loop phase noise measurement of the SAW resonator:

$$\alpha_R = \frac{f_m S'_{\phi R}(f_m)}{(2Q_L f_o)^2}. \tag{17}$$

If we define a new parameter $k_1$ to be $f_m S'_{\phi R}(f_m)$, from (17) and the fact that $Q_L = \pi f_o \tau_g$ we can combine the first two terms of (1) as a single term and rewrite (1) as

$$S_\phi(f_m) = \left[\frac{k_1 + \alpha_E}{(2\pi\tau_g)^2 f_m^3}\right] + \left[\frac{k_1}{(2\pi\tau_g) f_m^2}\right] + \left[\frac{2GFKT/P_o}{(2\pi\tau_g)^2 f_m^2}\right] + \frac{\alpha_E}{f_m} + \frac{2GFKT}{P_o}. \tag{18}$$

The constant $k_1$ is found in the same way as is $\alpha_E$—it is just the open-loop phase noise value at a 1 Hz offset—and it has the same relative magnitude as $\alpha_E$: $10^{-12}$. Expression (18) illustrates a fact pointed out by Parker [4, p. 104], that either the resonator or the amplifier may dominate the (close-in) phase noise response, and that for a given $\alpha_R$ the loaded $Q$ may affect which component dominates, since $k_1 = (2Q_L f_o)^2 \alpha_R$. The fact that $\alpha_R$ and $\alpha_E$ have a similar effect on phase noise is further discussed in the next section.

If one wishes to predict the open-loop phase noise response for the SAW resonator, (18) may be used to optimize for a value of $k_1$; the predicted phase noise to carrier ratio, $\mathcal{L}_R(f)$, at a 100 Hz offset (for example) is then given by $[10\cdot(\log(0.5k_1)-2)]$ dBc/Hz.

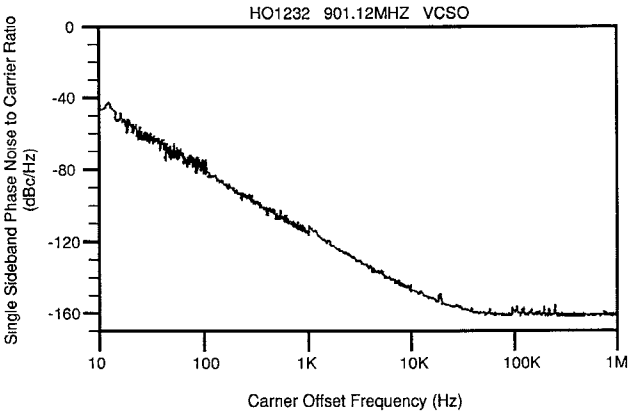


Fig. 2. Phase noise measurement of 0.9 GHz VCSO.

## III. Example of the Technique

Fig. 2 illustrates a phase noise measurement of a 0.9 GHz voltage-controlled SAW oscillator (VCSO) stabilized using an RF Monolithics SAW device which has a typical group delay of 1 $\mu$s and a loaded $Q$ of 2831. The compressed power gain of the loop amplifier was measured to be 12.0 dB and the carrier power level at the output of the VCSO loop amplifier is 16 dBm.

The phase noise measurements in Fig. 2 were made using a two-source technique such that the measured data shown reflect the actual noise of the oscillator being tested. The VCSO under test uses a SAW device which was 50 $\Omega$ matched to the loop amplifier in-band; resistive padding at the input and output of the loop amplifier provided control of the out-of-band SAW impedance variations. Note also the significant out-of-band SAW attenuation (Fig. 1), which results in large loop loss outside the operating frequency range.

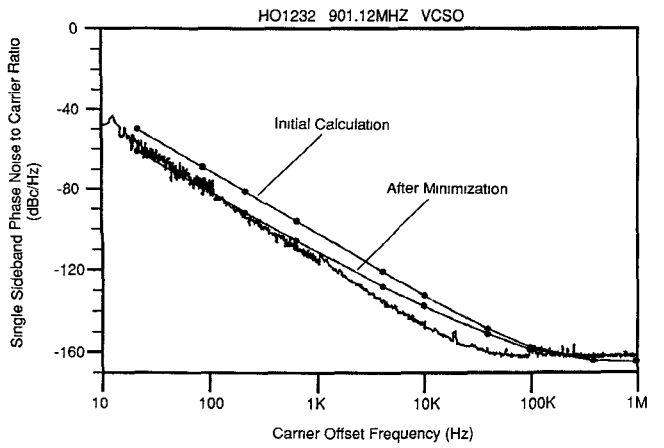


Fig. 3. Comparison of calculated phase noise characteristic with measured data.

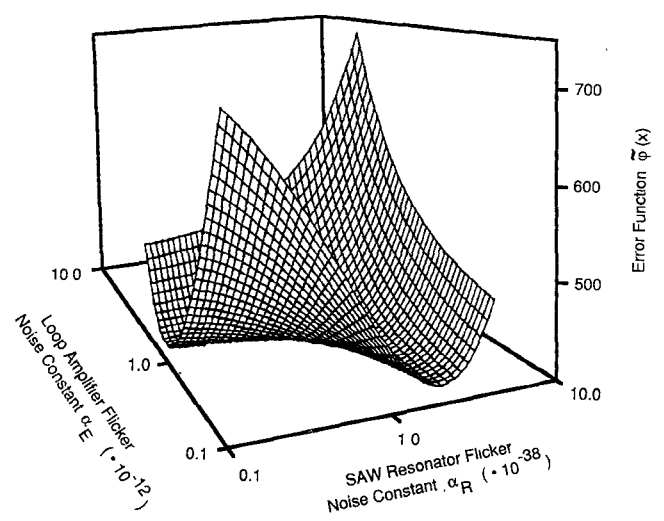


Fig. 4. Error function magnitude plotted versus flicker noise constants $\alpha_R$ and $\alpha_E$.

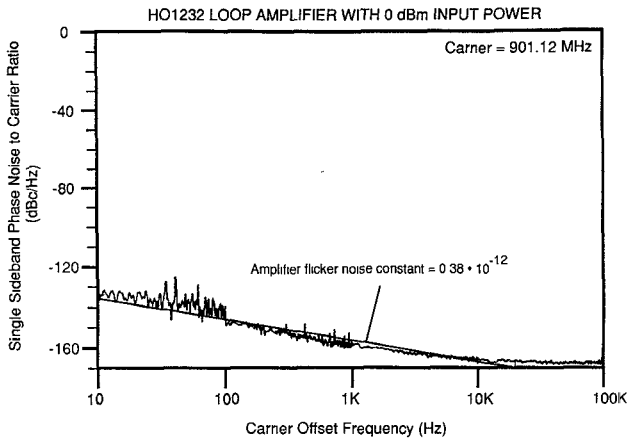


Fig. 5. Open-loop amplifier phase noise measurement.

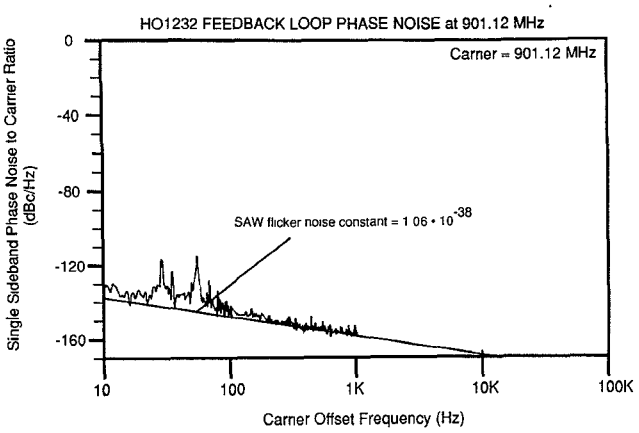


Fig. 6. Open-loop SAW phase noise measurement.

Initial values for the flicker noise constants for the SAW device and for the loop amplifier were chosen to be $\alpha_E = 3.0 \cdot 10^{-12}$ rad$^2$/Hz$^2$ and $\alpha_R = 11.5 \cdot 10^{-38}$ rad$^2$/Hz$^2$, and the noise factor $F$ was estimated to be 60 (17.8 dB). Fig. 3 illustrates the results of our minimization of (8); the summation in (8) ranged over 10 offset frequencies from 20 Hz to 1 MHz. The parameter vector $\boldsymbol{x}$ consisted of the parameters $F$, $k_1$ (or $\alpha_R$), and $\alpha_E$ as quantities to be varied. Upon completion of the minimization, the noise factor, $F$, did not change significantly from its initial value of 60, but $\alpha_R = 1.06 \cdot 10^{-38}$ and $\alpha_E = 0.38 \cdot 10^{-12}$ as final values. For this example, the steepest-descent technique was adequate to determine the approximate function minimum, and the iteration was stopped when the error function did not appreciably decrease in value from iteration to iteration.

A better fit to the measured data results if $\tau_g$ is included as a parameter in $\boldsymbol{x}$. Unfortunately, the optimum value for $\tau_g$ for minimizing the squared error tends to unreasonably high values and thus $\tau_g$ was omitted from the parameter vector. The source of this numerical problem is probably due to the high sensitivity of the objective function (8) to this parameter. This illustrates the well-established fact that a minimization approach to parameter determination requires careful attention to prevent unreasonable solutions for the parameter vector, particularly in our case if inaccuracy exists in the data for offset frequencies far from the carrier. We expect that by applying a suitable frequency-dependent weighting function in (8), we can reduce problems which arise from uncertainty in the data values far from the carrier. Another common technique is to apply bounds on the parameter vector $\boldsymbol{x}$ to prevent unreasonable numerical solutions.

It is interesting to view the error function behavior as a function of the parameters $\alpha_R$ and $\alpha_E$. Fig. 4 illustrates the magnitude of the error function as $\alpha_R$ and $\alpha_E$ are logarithmically varied over a wide range; note that the flat valley confirms the observation made in the previous section that each of these two parameters can have a similar effect on phase noise behavior. In order to assess the accuracy of our minimization, we plotted a straight $-10$ dB/decade line ($\alpha_R$ or $\alpha_E$ = constant) on carefully measured open-loop phase noise characteristics for the SAW resonator and for the loop amplifier, shown in Figs. 5 and 6; the agreement is good. The data in the open-loop phase noise measurement for the SAW device were omit-

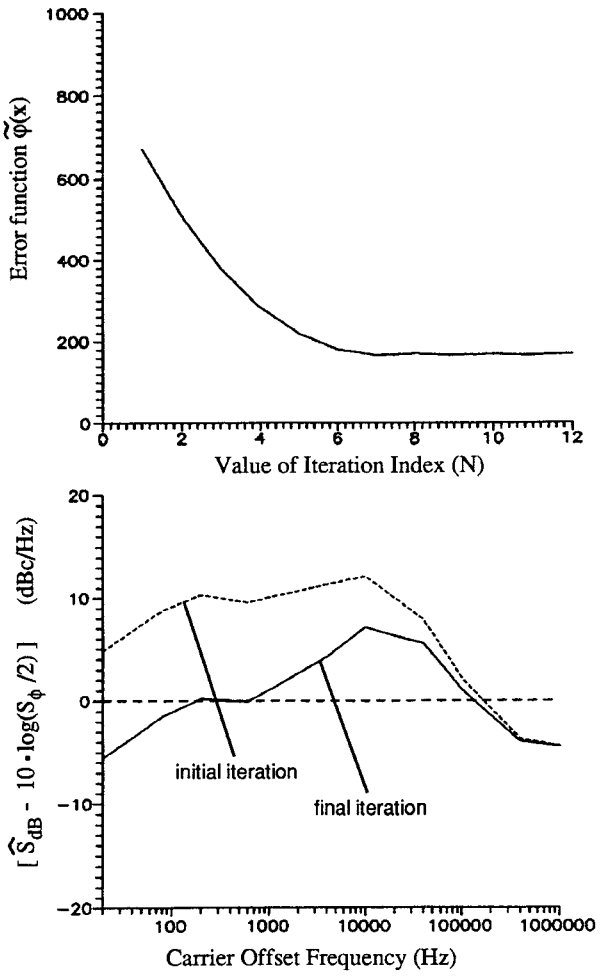


Fig. 7. Iteration history and comparison of initial/final discrepancy between calculated and measured phase noise to carrier ratio.

ted for frequencies beyond a 1 kHz offset because the measurement system loses phase track for these frequencies. Because the determination of $\alpha_R$ may be difficult for narrow-band passive devices which exhibit significant loss, a minimization approach may be an alternative, inexpensive technique for determining this flicker noise constant; in this case $\alpha_E$ may be omitted from the parameter vector $\boldsymbol{x}$.

We conclude by illustrating the iteration history for the minimization on the 0.9 GHz VCSO. Fig. 7 depicts the error function $\tilde{\varphi}(\boldsymbol{x})$ as a function of iteration index as the minimization progresses. The minimum value is approached after seven iterations, which is a typical result. The lower plot in Fig. 7 illustrates the difference between calculated and measured phase noise to carrier ratio as a function of offset frequency, for the final (ninth) iteration. The improvement resulting from the minimization is evident.

## IV. Conclusions

Determination of the parameter values which relate to the phase noise performance of a VCSO can be accomplished by minimizing a squared-error function which represents the difference between calculated and measured values of phase noise to carrier ratio. An expression developed by Parker is employed in the calculation of the double-sideband phase noise values.

As in any minimization scheme, care must be employed to prevent nonphysical or meaningless solutions for the parameter vector which is to be determined. To prevent difficulty, attention should be paid to the following considerations: (i) proper choice of parameters which comprise $\boldsymbol{x}$ and numerical bounds which constrain $\boldsymbol{x}$; (ii) specific choice of minimization scheme (steepest-descent with damping versus Newton–Raphson, for instance); (iii) accurate acquisition of original measurement data; and (iv) appropriate weighting of the error function which is to be minimized. Our numerical findings suggest that useful results can be obtained in the determination of VCSO circuit parameters.

## Acknowledgment

The authors wish to thank M. Robinson and A. Northam for helpful technical discussions and for their support of this joint industry/university research effort. They also acknowledge and appreciate helpful comments from an anonymous reviewer which have served to improve the manuscript.

## References

[1] T. E. Parker, "$1/f$ frequency fluctuations in quartz acoustic resonators," *Appl. Phys. Lett.*, vol. 46, no. 3, pp. 246–248, Feb. 1, 1985.
[2] V. F. Kroupa, "The state of the art of flicker frequency noise in BAW and SAW quartz resonators," *IEEE Trans. Ultrason., Ferroelectrics. Freq. Contr.*, vol. 35, pp. 406–420, May 1988.
[3] R. L. Baer, "Phase noise in surface-acoustic-wave filters and resonators," *IEEE Trans. Ultrason., Ferroelectrics, Freq. Contr.*, vol. 35, pp. 421–425, May 1988.
[4] T. E. Parker, "Characteristics and sources of phase noise in stable oscillators," in *Proc. 41st Annu. Freq. Contr. Symp.*, 1987, pp. 99–110.
[5] G. K. Montress, T. E. Parker, M. J. Loboda, and J. A. Greer, "Extremely low-phase-noise SAW resonators and oscillators: Design and performance," *IEEE Trans. Ultrason. Ferroelectrics, Freq. Contr.*, vol. 35, no. 6, pp. 657–667, Nov. 1988.
[6] T. E. Parker, and G. K. Montress, "Precision surface-acoustic-wave (SAW) oscillators," *IEEE Trans. Ultrason., Ferroelectrics, Freq. Contr.*, vol. 35, pp. 342–364, May 1988.
[7] G. Dahlquist, Å. Björck, and N. Anderson (translator), *Numerical Methods*. Englewood Cliffs, NJ: Prentice-Hall, 1974, ch. 10.
[8] *Low Phase Noise Applications of the HP8662A and HP8663A Synthesized Signal Generators*, Hewlett-Packard Company, Application Note 283-3, Dec. 1986.
[9] *Phase Noise Characterization of Microwave Oscillators — Phase Detector Method*, Hewlett-Packard Company, Product Note 11729B-1, Mar. 1984.
[10] *Phase Noise Characterization of Microwave Oscillators — Frequency Discriminator Method*, Hewlett-Packard Company, Product Note 11729C-2, Sept. 1985.
[11] D. B. Leeson, "A simple model of feedback oscillator noise spectrum," *Proc. IEEE*, vol. 54, pp. 329–330, Feb. 1966.

**David P. Klemer** (S'76–M'82) received the B.S.E., M.S.E., and Ph.D. degrees in electrical engineering from the University of Michigan in 1977, 1978, and 1982, respectively.

From 1983 to 1984 he was a staff member at MIT Lincoln Laboratory, Lexington, MA. He joined the Steinbrecher Corporation, Woburn, MA, in 1984; his work there involved millimeter-wave IMPATT power amplifiers and combiners, frequency multipliers, and other passive millimeter-wave circuits. In August 1988 he became an Assistant Professor in the Department of Electrical Engineering at the University of Texas at Arlington, where he is affiliated with the NSF/Center for Advanced Electron Devices and Systems. His present research activities involve GaAs devices and circuits for microwave and millimeter-wave applications to 100 GHz.

Dr. Klemer is a member of Sigma Xi, Phi Kappa Phi, Eta Kappa Nu, and Tau Beta Pi.

**Ko-Ming Shih** (S'87–M'90) received the B.S. degree from National Taiwan Normal University in 1976, the M.A. degree in physics from Washington University in 1983, the M.S. degree in electrical engineering from Louisiana State University in 1985, and the Ph.D. degree from the University of Texas at Arlington in 1990.

From 1985 to 1990 he was a research assistant in the NSF/Center for Advanced Electron Devices and Systems at the University of Texas at Arlington. He is now an Assistant Professor in the Department of Electrical and Computer Engineering, Mercer University, Macon, GA, where his research interests include semiconductor device modeling and characterization.

Dr. Shih is a member of Tau Beta Pi.

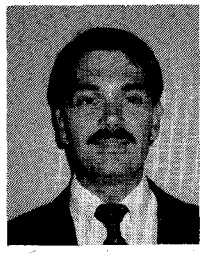

**Earl E. Clark III** (S'89–M'90) received the B.S.E.E. degree from the University of Texas at Arlington in May 1990.

After finishing military service, in 1983, he began work at RF Monolithics, Inc., Dallas, TX, as an RF engineering technician. In 1989 he became an RF Design Engineer in the Frequency Sources Department at RF Monolithics, where he is currently involved in the design of SAW-resonator-based oscillators.